

FRIDA JERNSTRÖM

Self-assembled monolayers  
of alkanethiols: A study of  
surface composition,  
wettability, and adsorption  
of proteins and peptides

Master's degree project



**Molecular Biotechnology Programme**  
**Uppsala University School of Engineering**

<b>UPTEC X 01 012</b>		<b>Date of issue 2001-02</b>
Author <b>Frida Jernström</b>		
Title (English) <b>Self-assembled monolayers of alkanethiols: A study of surface composition, wettability, and adsorption of proteins and peptides</b>		
Title (Swedish)		
Abstract Self-assembled monolayers (SAMs) of alkanethiols on gold were produced and characterised using contact angle goniometry, ESCA, SPR, and MALDI-MS. Two-component SAMs of polar and non-polar alkanethiols were included in the study. An alkanethiol equipped with an aromatic tail group was synthesised, and surface synthesis was carried out on hydroxyl-presenting SAMs to introduce fluorinated and aromatic tail groups respectively.		
Keywords Self-assembled monolayer, alkanethiols, surface synthesis, protein adsorption, peptide adsorption, SPR, MALDI-MS		
Supervisors <b>Helene Dérand, Gyros AB</b>		
Examiner <b>James Van Alstine, KTH</b>		
Project name	Sponsors	
Language <b>English</b>	Security	
<b>ISSN 1401-2138</b>	Classification	
Supplementary bibliographical information	Pages <b>36</b>	
<b>Biology Education Centre</b> Box 592 S-75124 Uppsala	Biomedical Center Tel +46 (0)18 4710000	Husargatan 3 Uppsala Fax +46 (0)18 555217

# **Self-assembled monolayers of alkanethiols: A study of surface composition, wettability, and adsorption of proteins and peptides**

**Frida Jernström**

## **Sammanfattning**

Vid hantering av små mängder vätska i miniaturiserade kanaler är kanalväggarnas egenskaper av stor betydelse. Man vill till exempel ha kanaler som tål alla sorters vätskor, och där molekyler som man vill analysera inte fastnar på väggarna. Ett sätt att påverka dessa egenskaper är att täcka väggytan med ett skyddande lager av molekyler som förändrar ytan så att den till exempel blir mer hydrofil. En grupp av molekyler som ofta används i detta syfte är s-k-alkanantioler, som består av långa kolvätekedjor med en svavelvätegrupp i ena änden, och en s-k funktionell grupp i den andra. Alkantioler bildar spontant ett tätpackat lager på guldytor, med svavlet riktat inåt och den funktionella gruppen pekandes utåt. Genom att variera vilken typ av funktionell grupp som sitter på molekylens s-k-grupp kan man skapa ytor som har de egenskaper som man önskar. I det här examensarbetet har alkanantioler med olika funktionella grupper använts för att förändra guldytors egenskaper, framförallt med avseende på adsorption av biomolekyler.

**Examensarbete 20 p på Molekylär bioteknik programmet**

**Uppsala universitet Februari 2001**

## Table of contents

<b>1 Introduction</b>	<b>1</b>
1.1 Aim of the study	1
<b>2 Theory</b>	<b>3</b>
2.1 Self-assembled monolayers	3
2.2 Contact angle measurements	5
2.3 ESCA	6
2.4 Surface Plasmon Resonance	6
2.4.1 Basic theory of Surface Plasmon Resonance	6
2.4.2 BIAcore instrumentation	7
2.5 MALDI-MS	7
<b>3 Materials and methods</b>	<b>9</b>
3.1 Preparation of self-assembled monolayers	9
3.1.1 Materials	9
3.1.2 TLI cleaning method	9
3.1.3 Plasma cleaning method	9
3.1.4 Adsorption of alkanethiols	10
3.1.5 Preparation of mixed SAMs	10
3.2 Synthesis of 11-phenoxy-1-mercaptoundecane	10
3.2.1 Materials	10
3.2.2 Method	10
3.3 Synthesis of heptafluorobutoxy mercaptoundecane	11
3.3.1 Materials	11
3.3.2 Method	11
3.4 Introduction of hydrophobic tail groups on hydroxylated SAMs	12
3.4.1 Surface synthesis with benzylbromide	12
3.4.2 Surface synthesis with heptafluoropropyl iodide	12
3.4.3 Surface synthesis with fluorinated anhydrides	13
3.5 Characterisation methods	13
3.5.1 Contact angle measurements	13
3.5.2 ESCA analysis	14
3.5.3 SPR	14
3.5.4 MALDI-MS	15
<b>4 Results and discussion</b>	<b>16</b>
4.1 Synthesis of alkanethiols with hydrophobic tail groups	16
4.1.1 Synthesis of 11-phenoxy-1-mercaptoundecane	16
4.1.2 Synthesis of heptafluorobutoxy mercaptoundecane	18
4.2 Introduction of hydrophobic tail groups on hydroxylated SAMs	18
4.2.1 Introduction of aromatic tail groups	18

4.2.2 <i>Introduction of fluorinated tail groups</i> .....	19
4.3 Mixed monolayers of hydrophilic and hydrophobic alkanethiols .....	21
4.4 Characterisation of produced SAMs .....	23
4.5 Adsorption of proteins and peptides .....	24
4.5.1 <i>Protein adsorption studied with SPR</i> .....	24
4.5.2 <i>Peptide adsorption studied with SPR</i> .....	26
4.5.3 <i>Peptide adsorption studied with MALDI-MS</i> .....	28
<b>5 Conclusions</b> .....	<b>31</b>
<b>6 Proposed future actions</b> .....	<b>32</b>
<b>7 Acknowledgements</b> .....	<b>33</b>
<b>References</b> .....	<b>34</b>

# 1 Introduction

This study was carried out at Gyros AB, the integrated microfluidics company developing a system for the integration of numerous bioanalytical processes on a CD with microscopic flow channels. By spinning the CD, nanoliters of liquids can be transported in a controlled fashion by means of centripetal force.

Sample handling and processing in microfluidic systems involve capillary forces and hydrodynamics that are directly affected by surface wettability. Furthermore, the volume to surface ratio of microsystems is very large, making surface chemistry of crucial significance. Control over non-specific adsorption of biomolecules is another important challenge if the microsystem is to be useful in the processing and analysis of biological samples. The location of the surface in the processing chain, as well as the application are factors determining the required surface characteristics and functionalities. For example, while non-specific adsorption of biomolecules must be minimised in flow channels near the sample injection site, surfaces downstream may be modified to serve as high affinity capture sites for biomolecules.

In the field of biotechnology much effort has been devoted to research concerning surface coatings with the potential to present a diverse number of functionalities. The spontaneous self-assembly of thin films of functionalised long-chain organic molecules has emerged as a promising method for effective and stable surface functionalization. The resulting self-assembled monolayers (SAMs) are well organised, with good coverage of the underlying surface and a number of possibilities of further modifications once formed. SAMs can be prepared using a wide range of different molecules and substrates, such as alkylsiloxanes, fatty acids and organosulfur compounds. The process of self-assembly of alkanethiols ( $\text{HS}(\text{CH}_2)_n\text{X}$ ) or disulphides ( $[\text{S}(\text{CH}_2)_n\text{X}]_2$ ) is by far the most studied, using gold as the solid substrate [1]. Mixed SAMs of alkanethiolates on gold have been constructed and shown to resist non-specific adsorption of proteins, or to promote biospecific adsorption of specific proteins [2, 3]. SAMs have also been used for covalent immobilisation of biomolecules (such as antibodies) onto the surface [1, 4]. Dextran modified SAMs are utilised in biointeraction analysis with surface plasmon resonance (SPR) [5]. Another area of application is MALDI-MS, where reversible binding of polypeptides to hydrophobic SAMs has been used to obtain sample de-salting and enrichment [6].

## 1.1 Aim of the study

The aim of the present study was to produce self-assembled monolayers (SAMs) of alkanethiols on gold, and to characterise the formed SAMs in terms of water-air contact angles, and protein and peptide adsorption.

The studied alkanethiols include commercially available substances of varying chain length and tail group polarity, as well as an alkanethiol with an aromatic tail group that was synthesised in the present study. To cover a wide range of contact angles, two-component monolayers of alkanethiols presenting polar and non-polar tail groups respectively were also produced and characterised.

To demonstrate how SAMs may be modified once formed, fluorinated and aromatic tail groups respectively were introduced on the surface of SAMs formed from hydroxylated alkylthiols. Wettability measurements were performed using contact angle goniometry. ESCA was used to analyse components of the SAM. Protein and peptide adsorption was measured using SPR and MALDI-MS.

## 2 Theory

### 2.1 Self-assembled monolayers

Self-assembly is the spontaneous organisation of molecules into stable, well-defined structures by non-covalent forces. During self-assembly, the species being deposited can interact predominately with the solid surface, and/or either the solvent or other, neighbouring molecules in solution. In the case of the SAMs discussed in the present report, the principle is quite simple: a molecule, essentially an alkane chain of typically 10-18 units, is equipped with a thiol (S-H) head group with a strong preferential adsorption to the substrate, Au(111). The sulphur head groups generally bind to the gold as a thiolate ( $\text{Au-S}^-(\text{CH}_2)_n\text{X}$ ), forming a well-structured monolayer with the tail groups pointing outwards from the surface. Many different functional groups can thus be introduced at the surface under the constraints that a) they do not compete significantly with the thiol in the adsorption to the substrate, b) they do not react with thiols, and c) they are not too bulky to permit close packing of the hydrocarbon chains [7].

The key principle is that the final structure of a perfectly organised SAM is close to, or at thermodynamic equilibrium. It therefore tends to assemble spontaneously and relax in that structure, rejecting defects. Studies of the Au-S interaction have shown that the sulphur of *n*-alkanethiols, ( $\text{HS}(\text{CH}_2)_n\text{CH}_3$ ),  $n > 10$ , bind at threefold hollow sites at the Au(111) crystal net-work, forming a symmetrical structure, with a nearest neighbour distance of about  $5\text{\AA}$  [8]. The overall adsorption energy, typically in the range of 35-45 kcal/mole, is contributed to by the strong sulphur-gold interaction. As is indicated in figure 1, the molecules assemble in a slightly tilted, all *trans* configuration. It is the slight mismatch between the pinning distance and the van der Waals diameter of the alkyl chain that forces the molecules to tilt in order to optimise the lateral interactions between molecules within the monolayer. Varying degrees of crystallinity (all *trans* in nature) are obtained depending on the alkylic chain length [1]. The longer the chain, the more the all *trans* configuration becomes thermodynamically favourable. As a rule of thumb, alkanethiols with chains shorter than 10-12 methylene units form rapidly increasing fractions of *gauche* conformers, located at the outermost portion of the alkyl chain. The all *trans* configuration is preferable from a surface chemist's point of view because of its higher homogeneity and superior surface coverage.

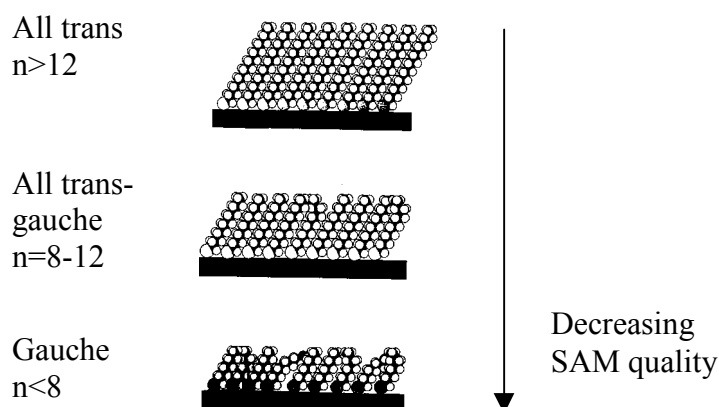


**Figure 1.** Chain length dependence of SAM organisation (*n* denotes number of alkylic groups in the chain). [1]

Organosulphur SAMs are usually prepared by immersing the substrate in an organic or aqueous solvent containing the adsorbing species (figure 2). Gold is often a preferable substrate because of its high inertness, but well-organised SAMs have been produced on other metal surfaces such as silver or copper [9, 10]. Ethanol is commonly used as solvent due to its low cost, low toxicity, and availability in high purity. The initial adsorption takes place within seconds and is followed by an organisation phase, which should be allowed to continue for >15h for complete monolayer formation.

Disulphides undergo S-S bond dissociation, adsorbing on the surface as two separate alkanethiolate species. The adsorption kinetics of disulphides has been shown to be slower than for the corresponding thiols [7, 11]. Since the transformation of thiols into disulphides readily occurs in the presence of oxygen this should be taken into consideration, especially when producing multi-component SAMs through the competitive adsorption of different alkanethiol species.

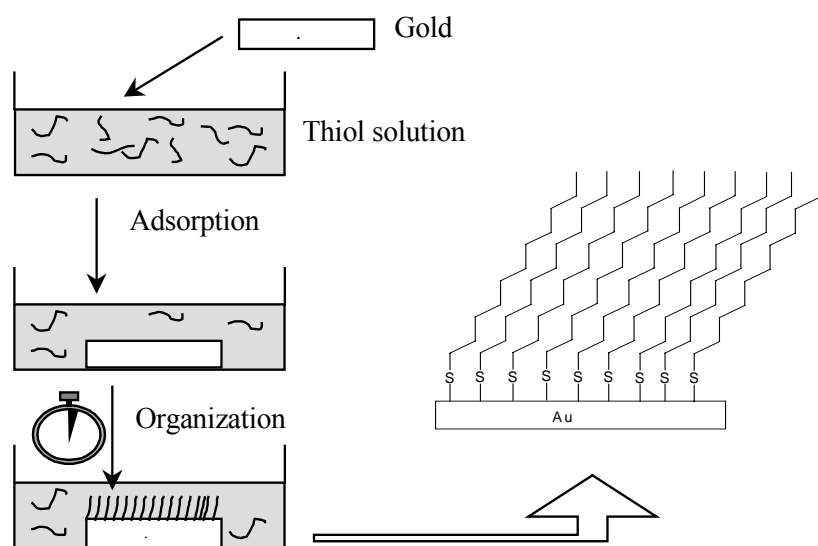


**Figure 2.** Adsorption of alkanethiols on an Au substrate surface.

The properties of an alkanethiolate SAM formed on gold primarily depend on the immersion time, the solvent used, the purity of the thiol, the temperature, and on the quality of the gold substrate [1]. The roughness and cleanliness of the immersed substrate is of crucial importance for the quality of the monolayer. There are a variety of techniques for cleaning the surface before depositing the SAM. These include exposure to a powerful oxidizing mixture of concentrated sulphuric acid and hydrogen peroxide (Pirahna solution) [1], and the less aggressive TL1-solution comprising of hydrogen peroxide, ammonium and water [12]. Dry cleaning methods include UV/ozone treatment, and etching in O<sub>2</sub> or Ar plasma. Dry techniques, such as plasma treatment, are preferable when using chemically sensitive substrate supports, such as polymers.

Gold surfaces oxidise when treated with oxygen plasma. This may affect the properties of a self-assembled monolayer (SAM) formed on the surface [13]. To avoid any such influence the gold oxide can be reduced by reaction with ethanol [14].

## 2.2 Contact angle measurements

A drop of liquid that is put on a solid surface will modify its shape under the pressure of the different surface/interfacial tensions, until reaching equilibrium. The three-phase equilibrium is described by Young's equation (1), where  $\gamma_{ij}$  is the surface tension between  $i$  and  $j$ , subscripts  $v$ ,  $l$  and  $s$  refers to vapour, liquid and solid respectively, and  $\theta$  is the equilibrium contact angle (figure 3).

$$\cos\theta = \frac{\gamma_{sv} - \gamma_{sl}}{\gamma_{lv}} \quad (1)$$

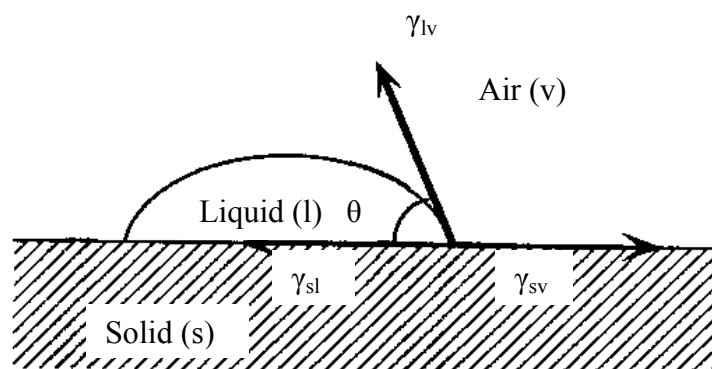


**Figure 3.** The three-phase equilibrium.  $\gamma_{ij}$  is the surface tension between  $i$  and  $j$ , subscripts  $v$ ,  $l$  and  $s$  refers to vapour, liquid and solid respectively, and  $\theta$  is the equilibrium contact angle.

The contact angle is a quantitative measure of the wettability of a surface, e.g. the contact angle of water is a strong function of the hydrophilicity of the surface. A commonly used method for contact angle measurement is the sessile drop technique, where a droplet of liquid is placed on the solid surface using a syringe or a micropipette. The droplet is observed through a low magnification microscope, and the resulting contact angle is measured using a goniometer fitted in the eyepiece. Advancing ( $\theta_a$ ) and receding ( $\theta_r$ ) contact angles are the angles measured during the expansion and retraction of the droplet respectively. The difference ( $\theta_a - \theta_r$ ) is referred to as the hysteresis of the surface, and can provide information about surface homogeneity.

## 2.3 ESCA

Electron spectroscopy for chemical analysis (ESCA), also known as X-ray photoelectron spectroscopy (XPS) is a method for characterising the few outermost atomic layers at the surface of a solid. Not only does ESCA analysis give quantitative information about the elemental composition of a surface (C, O, N etc.), it can also provide information about the chemical environment, geometry, and orientation of the chemical species at the surface.

ESCA is based on the principle of photoemission, where an x-ray photon incident on a sample can ionise an atom, producing an ejected free electron. The kinetic energy  $E_K$  of the emitted photoelectron depends on the photon energy  $h\nu$ , as expressed by the Einstein photoelectric relation (2).

$$E_K = h\nu - E_B \quad (2)$$

$E_B$  is the binding energy of the electron to the atom concerned. The value of  $h\nu$  is known, and a measure of  $E_K$  consequently determines  $E_B$ . Since the binding energies of the electrons have values that are distinct for each atom, the calculated values of  $E_B$  serve as a fingerprint for the identification of the atom. However, the efficiency of the spectrometer detector is dependent of the kinetic energy of the emitted electron, resulting in a higher sensitivity for some elements than for others. To reflect this difference, each element is assigned an atomic sensitivity factor (ASF), normalised so that fluorine has an ASF of 1.00.

## 2.4 Surface Plasmon Resonance

### 2.4.1 Basic theory of Surface Plasmon Resonance

Interaction phenomena at surfaces can be monitored in real time, i.e. under continuous flow conditions, using the method of surface plasmon resonance (SPR) detection. The surface plasmon oscillation is a strongly localised optical wave propagating along the interface between the metal and the surrounding medium. It occurs when plane-polarized light is reflected under flat angles from a thin metal film deposited on a glass substrate. At a specific angle, ( $\theta_m$ ) the photons interact with the free electron cloud in the metal film, causing a drop in the intensity of the reflected light. The angle at which this reflection minimum occurs is extremely sensitive to changes in the refractive index of the interfacial region near the metal surface, changes caused by for example the adsorption of biomolecules to the surface.

The most frequently used method for optical excitation of a surface plasmon is schematically shown in figure 4. It is often referred to as the Kretschmann configuration. The technique is sensitive to molecular events occurring in an interaction volume defined by the extension of the evanescent electric field of the surface plasmon, extending a few hundred nanometer into the ambient medium [15].

## 2.4.2 BIAcore instrumentation

In the BIAcore instrumentation, an optical detection unit based on SPR detection is combined with a chemically modified gold surface and a microfluidic cartridge for sample handling (figure 4) [5]. The monitoring of the resonance angle as a function of time is called a sensorgram and is used for direct observation and evaluation of binding and dissociation events at the sensor surface. To maximise the utilisation of the evanescent field, a three-dimensional matrix extending from the surface is commonly used in BIAcore applications. Using a two-dimensional surface, as is done in the present report, limits the maximal signal-to-noise sensitivity of the measurement.

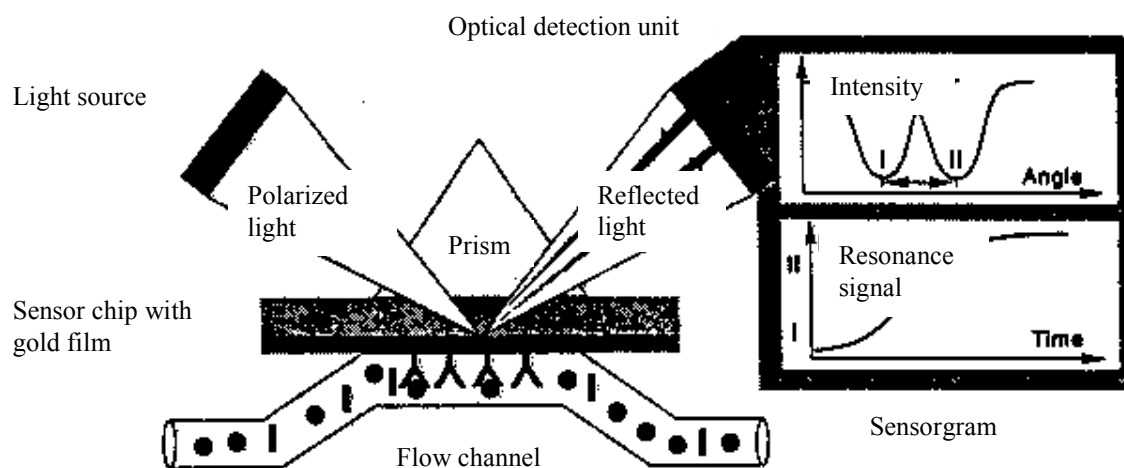


**Figure 4.** Schematic illustration of the SPR detection principle [5].

## 2.5 MALDI-MS

In a mass spectrometer (MS) molecules in the gaseous state under low pressure are bombarded with a beam of high-energy electrons. This can result in the dislocation of one of the electrons of the molecule, producing a positively charged molecular ion. Soon after they are formed, most of the molecular ions undergo fragmentation, producing several new cations. The way a molecular ion is fragmented depends on the nature of the particular molecular ion, and can provide useful information about the structure of a complex molecule. The ions are accelerated and directed through a curved tube, passing through a variable magnetic field. The magnetic field influences the path of the moving ions. Depending on the strength of the magnetic field at a given moment, only ions with a specific  $m/z$  ratio will follow a path that has the required curvature for the ion to pass through the tube and be registered by the ion detector. The intensity of the ion beam reaching the detector is simply a measure of the relative abundance of ions with a particular  $m/z$  ratio. Since the charge on all of the ions is +1, the ions are sorted on the basis of their mass.

Matrix-assisted laser desorption/ionisation mass spectrometry (MALDI-MS) is one of the most sensitive mass spectrometry approaches. The detection limit lies in the attomole to nanomole range. MALDI sample preparation is performed by drying a mixture of sample and matrix on the MALDI probe surface. Ionisation of the analyte is achieved by focusing a pulse of laser light onto the sample-matrix preparation. First, the matrix is ionised. Energy and protons are then transferred from the matrix to the analyte, which in turn is ionised.

## 3 Materials and methods

### 3.1 Preparation of self-assembled monolayers

#### 3.1.1 Materials

1H-1H-2H-2H-Perfluorodecanethiol	(97%, ABCR AV20176)
Octadecylmercaptan	(98%, Aldrich O185-8)
1-Hexadecanethiol	(92%, Aldrich H763-7)
1-Undecanethiol	(98%, Aldrich 51.046-7)
11-Mercaptoundecanoic acid	(95%, Aldrich 45.056-1)
11-Mercapto-1-undecanol	(97%, Aldrich 44.752-8)
11-Phenoxy-1-mercaptoundecane	(Synthesised in this study)

Solvents: Ethanol (95%, Kemetyl)

TL1: Ammonium solution (25%, Riedel-de Haën 3051)  
Hydrogen peroxide (30%, Merck 12201-1)

Gasses: Oxygen (O<sub>2</sub>), Nitrogen (N<sub>2</sub>)

Substrate support: Polycarbonate (PC) and Zeonex CD discs, injection molded at Åmic, Uppsala, and microscope slides (glass, Merck 101474-0)

Substrate surface: Evaporation of gold films on the substrate supports was carried out at Åmic, Uppsala. A 40 nm layer of chromium (Cr) was evaporated on the PC substrate support, followed by evaporation of a 400 nm gold film on the Cr layer. On the Zeonex and glass surfaces 40 nm of titanium (Ti) was evaporated on the substrate support, followed by evaporation of a 75 nm gold film on the Ti layer. The SAMs used in the SPR measurements were prepared on gold covered sensor chips (SIA Kit Au, Biacore BR-1004-05).

#### 3.1.2 TL1 cleaning method

All tweezers and spoons used in the handling of alkanethiols and gold surfaces were cleaned with TL1 solution (1:1:5 solution of NH<sub>3</sub>, H<sub>2</sub>O<sub>2</sub> and H<sub>2</sub>O) 5min at 80°C, rinsed rigorously with water, and blown dry with N<sub>2</sub> prior to use.

#### 3.1.3 Plasma cleaning method

Previous to any treatment all surfaces were placed in a plasma reactor (Plasma Science PS0500) on a glass support 21cm from the chamber floor. After evacuation to a base pressure of 30 mTorr, oxygen was let in and the gas flow adjusted to the desired level of 10sccm. The RF power used was 100W and the plasma treatment time was 5 minutes. The reactor chamber was then vented with ambient air. To reduce oxidised gold, all surfaces were immersed in ethanol for 20 minutes with gentle shaking before further usage.

### 3.1.4 Adsorption of alkanethiols

The alkanethiol was dissolved in ethanol that had been degassed with N<sub>2</sub> for 30 minutes. Thiol concentrations used in this study were in the range of 1-2 mM. In some cases, ultrasonication of the solutions was needed for the thiol to dissolve. Plasma treated gold surfaces were left in the thiol solution at room temperature for 15-72 h. The surfaces were ultrasonicated in ethanol for 1-2 minutes to remove any physisorbed species, and blown dry with N<sub>2</sub> prior to characterisation.

### 3.1.5 Preparation of mixed SAMs

Two-component solutions of 1-undecanethiol and 11-mercapto-1-undecanol in ethanol were prepared with the molar fraction in solution of the polar component ( $X_{\text{OH}}^{\text{SOL}}$ ) varying from 0 to 1. The total concentration of thiol was 1 mM in all solutions. Preparation of SAMs from these solutions was carried out as outlined above.

## 3.2 Synthesis of 11-phenoxy-1-mercaptoundecane

### 3.2.1 Materials

Phenol	(Aldrich 32.811-1)
Sodium	(Riedel-de Haën 31429)
11-Bromo-1-undecen	(Fluka 18640)
Thioacetic acid	(Sigma T-5375)
Sodium methoxide	(Aldrich 15625-6)
Acetic acid	(Merck 1.00063.1000)
Sodium chloride	(Merck 1.06404.1000)
Magnesium sulphate	(Merck 1.06067.1000)
$\alpha\alpha'$ -Azobisisobutyronitril (AIBN)	(Fluka 11630)
Solvents: Heptane	(Merck 1.04379.1000)
Diethyl ether	(Merck 1.00929.1000)
Silica gel 60	(Fluka 60752)
Silica gel TLC plates	(Fluka 60805)
TLC developing liquid, AMC:	6mM Cerium sulphate (Aldrich 35900-1)
	34mM Ammoniumheptamolybdat tetrahydrate (Fluka 09880)
	1.2mM Sulphuric acid (Merck 1.00731.1000)

### 3.2.2 Method

The method used in the synthesis of 11-phenoxy-1-mercaptoundecane has previously been described by Sigal et al [17].

Sodium (0.4g, 17mmol) was dissolved under nitrogen in methanol (40ml) that had been dried over 0.3nm molecular sieve. Phenol (2.1g, 20mmol) and 11-bromo-1-undecene (2.4g, 10mmol) were added sequentially, and the solution was heated under reflux for 17h under nitrogen. The solvent was evaporated to give a crude oil. Purification was carried out by silica gel flash chromatography using 75:1 heptane/ether, resulting in a clear oil (1.8g). The subsequent thin layer chromatography (TLC) with 75:1 heptane/ether as eluent, and NMR analysis indicated the presence of 11-phenoxy-1-undecene without detectable by-products.  $^1\text{H-NMR}$  ( $\text{CDCl}_3$ , 270MHz,  $\delta$ ): 7.3 (m, 2H), 6.9 (m, 3H), 5.8 (m, 1H), 5.0 (m, 2H), 4.0 (t, 2H), 2.1 (m, 2H), 1.8 (m, 2H), 1.2-1.7 (m, 14H).

The 11-phenoxy-1-undecene was dissolved in dry tetrahydrofuran (40ml) together with thioacetic acid (1.5ml, 20mmol), and azobisisobutyronitrile (100mg, 0.6mmol). The solution was irradiated for 4h under a 500W medium-pressure Hg-lamp. The solvent was evaporated, resulting in a yellow-coloured oil. Hydrolysis to the thiol was carried out without further purification. The crude thioacetate was dissolved in 50ml of dry methanol. The solution was purged with nitrogen and a 2M solution of sodium methoxide (7.5ml, 15mmol) in methanol was added anaerobically. The solution was stirred under nitrogen for 15min at room temperature, and thereafter neutralized with acetic acid (2ml). Evaporation of the solvent gave an orange-coloured salt cake with brown spots, which was taken up in ether (50ml), washed with three portions of saturated NaCl solution (3x20ml), and dried over magnesium sulphate over night. Evaporation of the solvent, resulting in an orange-coloured oil, was followed by purification by flash chromatography on silica gel using 75:1 heptane/ether as the eluent. Evaporation gave the thiol (1.7g, 6mmol) as a clear oil that solidified at 4°C. TLC showed possible traces of phenol in the final product.

NMR of final product: Chloroform (700 $\mu\text{l}$ ) was added to 26mg of the 11-phenoxy-1-mercaptoundecane.  $^1\text{H-NMR}$  ( $\text{CDCl}_3$ , 270MHz,  $\delta$ ): 7.25 (m, 2H), 6.90 (m, 3H), 3.94 (t, 2H), 2.85 (t, 2H), 2.31 (s, 2H), 1.2-1.8 (m, 15H). (Appendix 1)

### **3.3 Synthesis of heptafluorobutoxy mercaptoundecane**

#### **3.3.1 Materials**

2,2,3,3,4,4,4-Heptafluoro-1-butanol (ABCR AV10414)

#### **3.3.2 Method**

The method used in the synthesis of heptafluorobutoxy-mercaptoundecane was identical to the method described in section 3.4.2, except for the following changes in the chemicals and quantities used: In the synthesis of heptafluorobutoxy-undecene, heptafluoro-1-butanol (2.5ml, 20mmol) reacted with 11-bromo-1-undecene (7ml, 30mmol). Due to low yield, the product from this synthesis could not be characterised with NMR.

### **3.4 Introduction of hydrophobic tail groups on hydroxylated SAMs**

#### 3.4.1 Surface synthesis with benzylbromide

##### 3.4.1.1 Materials

Benzylbromide	(Fluka 13250)
Heptafluoropropyl iodide	(ABCR AV14784)
Sodium hydride	(60%, Merck 8.145520100)
N-N dimethylformamide (DMF)	(Kebo 17134-1)
Gass: Argon (Ar)	

##### 3.4.1.2 Method

On a gold surface on a microscope slide glass support a SAM was prepared from an ethanol solution containing 1mM 11-mercapto-1-undecanol. The resulting hydroxyl-presenting surface exhibited a static contact angle of 10°, and was washed with ethanol and DMF prior to alkylation.

Sodium hydride (15mg, 0.63mmol) was dissolved in dry DMF (15ml), and the solution was purged with Ar. The hydroxyl presenting SAM surface was placed in the solution, and the temperature was raised to 60°C. The sodium hydride was allowed to react with the hydroxyl groups for 1h with gentle shaking, and under Ar-purge. Benzylbromide (20µl, 0.17mmol) was then added to the solution, and the reaction went on for 2h under the same conditions. The surface was ultrasonicated in DMF, ethanol, and deionised water for a total of 2 minutes.

#### 3.4.2 Surface synthesis with heptafluoropropyl iodide

##### 3.4.2.1 Materials

Heptafluoropropyl iodide	(ABCR AV14784)
Gass: Nitrogen (N <sub>2</sub> )	

##### 3.4.2.2 Method

On a gold surface on a microscope slide glass support a SAM was prepared from an ethanol solution containing 1mM 11-mercapto-1-undecanol. The resulting hydroxyl-presenting surface exhibited a static contact angle of 10°, and was washed with ethanol and DMF prior to alkylation.

Sodium hydride (24mg, 1.0mmol) was dissolved in dry DMF (15ml) and the solution was purged with N<sub>2</sub>. The hydroxyl presenting SAM surface was placed in the solution at room temperature.

The sodium hydride was allowed to react with the hydroxyl groups for 1h with gentle shaking, and under N<sub>2</sub> purge. Heptafluoropropyl iodide (5 $\mu$ l, 35 $\mu$ mol) was then added to the solution, and the reaction went on for 2h under the same conditions. The surface was ultrasonicated in DMF, ethanol, and deionised water for a total of 2 minutes.

### 3.4.3 Surface synthesis with fluorinated anhydrides

#### 3.4.3.1 Materials

Trifluoroacetic anhydride (TFAA)	(F <sub>3</sub> CC(O)OC(O)CCF <sub>3</sub> , Supelco 33165-U)
Heptafluorobutyric anhydride (HFAA)	(F <sub>3</sub> CF <sub>2</sub> CF <sub>2</sub> CC(O)OC(O)CF <sub>2</sub> CF <sub>2</sub> CF <sub>3</sub> , Supelco 33170-U)
Triethylamine (Et <sub>3</sub> N)	(Aldrich STO886)
Tetrahydrofuran (THF)	(Kebo 27428-1)
0.3nm Molecular sieve	(Merck 1.05704.1000)

#### 3.4.3.2 Method

Introduction of fluorinated tail groups was carried out using trifluoroacetic anhydride (TFAA) and heptafluorobutyric anhydride (HFAA) respectively. The method involving TFAA has previously been described by Lestelius et al [16].

On a gold surface on a microscope slide glass support a SAM was prepared from an ethanol solution containing 1mM 11-mercapto-1-undecanol. The resulting hydroxyl-presenting surface exhibited static contact angles of 10°, and was washed with ethanol and THF. The surface was then exposed to the anhydride (0.3 ml, 2.2mmol TFAA; 1.2mmol HFAA) in dry THF (30ml) in the presence of triethylamine (0.3ml) for 1h with gentle shaking, and under N<sub>2</sub> purge. This was followed by ultrasonication in THF, ethanol, and deionised water for a total of 2 minutes to remove physisorbed species.

## 3.5 Characterisation methods

### 3.5.1 Contact angle measurements

On all surfaces the static water contact angle ( $\theta_s$ ) was measured on a Ramé-Hart contact angle goniometer. A drop of water was placed on the surface using a micro-syringe. The needle was then removed from the liquid, and the contact angle noted. For measurement of advancing and receding angles the needle was left in contact with the liquid while the drop was expanded and retracted respectively. Advancing and receding contact angles were measured on some of the surfaces. For each sample the reported value is the mean calculated from two or more measurements at different places on the surface.

### 3.5.2 ESCA analysis

ESCA analysis was performed at Pharmacia, Uppsala, on a Perkin-Elmer Physical Electronics 5000LS X-ray photon-electron spectrometer equipped with a monochromatic Al K $\alpha$  source, operating at 15kV and 40mA, and an Apollo 4000 data system.

### 3.5.3 SPR

#### 3.5.3.1 Materials

BIAcore accessories: SIA Kit Au (Biacore BR-1004-05)  
BIAMaintenance Kit (Biacore BR-1002-22)

Proteins/peptides: bovine serum albumin (BSA) (US Biological Chemtec A1310)  
lysozyme from chicken egg white (Sigma L-6876)  
neuropeptide Y amide Fragment 1-24 (Sigma N-4896)  
angiotensin I (Sigma A-9650)  
Ile-Ser Bradykinin (Sigma B-1643)

Sodium hydroxide (Merck 1.06498.1000)  
di-Sodiumhydrogenphosphate (Merck 1.06586.0500)

#### 3.5.3.2 Method

SAMs were prepared from a 1mM ethanol solution of the respective alkanethiol on the gold covered sensor chips from the SIA Kit Au. After ultrasonication, all chips were blown dry with N<sub>2</sub>, and glued into the BIAcore cassette according to the manufacturer's instructions. The sensor chip was then docked to the BIAcore instrument (BIAcore 1000, Pharmacia Biosensor). Prior to each run, a cleaning procedure exposing the fluidics of the instrument to SDS was performed according to the manufacturer's instructions.

The running buffer PBS (0.15M NaCl, 20mM NaH<sub>2</sub>PO<sub>4</sub>, pH 7.2) was filtered through 22 $\mu$ m filter and degassed with N<sub>2</sub> before use. Buffer pH was adjusted with NaOH. Adsorption measurements were performed using different protein/peptide solutions in the parallel flow channels on the SAM-covered chip. The adsorption was measured at a flow rate of 5 $\mu$ l/min. Protein concentration was 1mg/ml in PBS for all samples, and peptide concentration was 0.1mg/ml of each peptide. Protein solutions were passed over the surface during a total of 48 to 78 minutes (8-13x30 $\mu$ l separated by 1 minute of PBS pH7.2). The adsorption time for the peptide solution was 12 minutes (2x30 $\mu$ l injections separated by 1 minute of PBS).

### 3.5.4 MALDI-MS

#### 3.5.4.1 Materials

Trypsine digest of bovine serum albumin (BSA), 4.75pmol/ $\mu$ l  
4-hydroxy- $\alpha$ -cyano-cinnamic acid, 4HCCA (Sigma C2020)

#### 3.5.4.2 Method

On gold surfaces on Zeonex support, MALDI-MS target circles ( $\varnothing \approx 2$ mm) were engraved using a sharp knife. On each surface a SAM was prepared from a 2mM ethanol solution of the respective alkanethiol. As a negative control, a bare gold surface on Zeonex support was plasma treated and placed in ethanol. After ultrasonication, all surfaces were blown dry with N<sub>2</sub> and placed onto a sheet of Al-foil with the Zeonex support facing the foil. A 1  $\mu$ l droplet of BSA-digest was placed on the MALDI-MS target circle. The droplet was left on the surface for 10min, or until evaporation of the drop began to be visible, i.e. after <3 min for the bare gold surface and the hydroxyl-presenting surface. 4 $\mu$ l of deionised water was then placed on the peptide droplet and left there for 10 min. Finally, the whole surface was washed rigorously with water and wrapped loosely in Al-foil. Before insertion into the mass spectrometer 1-2  $\mu$ l of matrix (70% ACN, 0.1% TFA, 1/4 saturated with 4HCCA) was applied onto the target circle. MALDI mass spectra were recorded on a Voyager-DE™ PRO Biospectrometry Workstation (PerSeptive Biosystems Inc.) operated in the positive-ion mode.

## 4 Results and discussion

Self-assembled monolayers (SAMs) can conveniently be produced from solution of alkanethiols. Therefore, the most important challenge in the preparation of SAMs most often lies in the limited availability of starting material, i.e. alkanethiols that are of the right length, and that are equipped with the right tail group to result in a surface exhibiting the desired properties. The commercially available long-chain alkanethiols are primarily limited to unsubstituted alkanethiols ( $\text{CH}_3(\text{CH}_2)_n\text{SH}$ ;  $n=0-18$ ), that form low-energy methyl surfaces, and substituted alkanethiols with carboxylic ( $-\text{COOH}$ ), or hydroxyl ( $-\text{OH}$ ) tail groups. Short-chain substituted alkanethiols ( $\text{X}(\text{CH}_2)_n\text{SH}$ ,  $n=1,2$ ,  $\text{X}=\text{NH}_2$ ,  $(\text{CF}_2)_n\text{CF}_3$ ) are also commercially available, but the produced SAMs may not be as highly organised as for the long-chain thiols. To obtain a broad selection of surface functionalities the desired substituted alkanethiols must therefore be synthesised from commercially available precursors, something that often involves several time consuming synthetic steps and difficult chromatographic separations. Alkylhalides are commonly used synthetic precursors for producing alkane thiols. Bromide and iodide, which are weak bases and therefore excellent leaving groups, provide useful reaction centres for the alkylation reaction. The thiol group is generally introduced in the final steps of the synthesis because of its sensitivity toward oxidation and incompatibility with various reagents. Photolytic addition of thioacetic acid with subsequent solvolysis is an effective method for the introduction of the thiol group.

Alternatively, functional groups can be introduced on the surface of already formed SAMs. This approach intuitively appears as the most convenient since it involves fewer and less time consuming steps than a complete synthesis. However, the efficiency of an on-surface synthesis can be affected by steric hindrance limiting the conversion of tail groups. Consequently, the control over the resulting surface composition is far greater if the entire substituted alkanethiol is synthesised and used for SAM formation. In the present study, both approaches have been attempted. The ambition was not to optimise the synthesis methods in terms of yield, but to produce a wide variety of surfaces with respect to functional groups and wettability to be tested regarding their affinity for proteins and peptides.

### 4.1 Synthesis of alkanethiols with hydrophobic tail groups

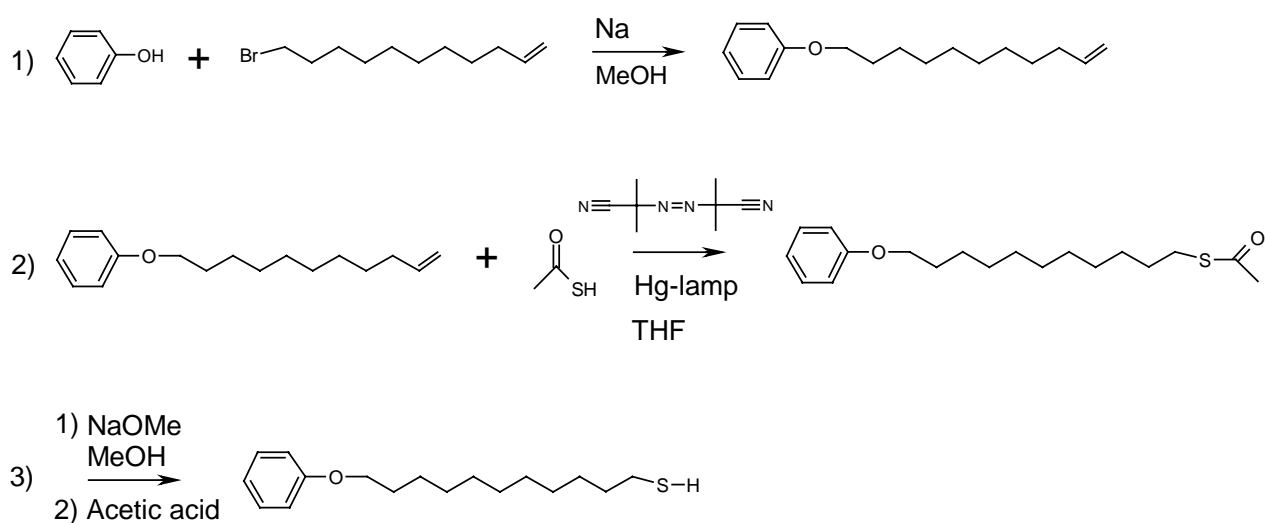
Synthesis of two substituted alkane thiols, equipped with aromatic and fluorinated tail groups respectively was attempted in this study. The aromatic thiol has previously been utilised for the formation of low-surface energy SAMs with high protein affinity [17]. Fluorinated alkane thiols have been shown to form intermediate- to low-surface energy SAMs [4, 7, 18].

#### 4.1.1 Synthesis of 11-phenoxy-1-mercaptoundecane

The synthesis of 11-phenoxy-1-mercaptoundecane is outlined in scheme 1. The yield from the synthesis was 60% as estimated by weighing the product, and the NMR measurement indicated that no by-products were present, but that the thiol had been oxidised to form the disulphide.

The resulting spectrum from the  $^1\text{H-NMR}$  analysis of the final product is found in appendix 1. The peaks in the spectrum are assigned numbers correlating them with the hydrogen atoms corresponding to the respective chemical shift. Triplets caused by signal splitting between the two adjacent hydrogen pairs next to the phenoxy- and disulphide groups respectively are expanded and shown in the offset plots. As was previously mentioned, thiols are readily oxidised to disulphides. Peak number 6 in appendix 1 corresponds to the hydrogens on each side of a disulphide bond, indicating an important fraction of disulphides in the final product (ca 35%). The presence of disulphides should not be a problem when preparing single-component SAMs with adsorption over night [11]. However, the solubility of disulphides is generally lower than for the corresponding thiol, something that was also observed in the present study.

SAMs were prepared from the synthesised 11-phenoxy-1-mercaptoundecane and the resulting surfaces had an average static contact angle of  $55^\circ$ , advancing contact angle of  $68^\circ$ , and a receding angle of  $35^\circ$ . The contact angles varied with as much as  $10^\circ$  between different SAM preparations. The resulting advancing contact angle is somewhat low compared to previously reported values of  $85^\circ$  for a SAM of 11-phenoxy-1-mercaptoundecane [17]. The relatively high hysteresis indicates that the surface is relatively heterogeneous. Furthermore, ESCA data of the same surface (table 1; -OPh) shows that sulphur is present on the surface, indicating that the monolayer is not completely covering the surface, or that the product is impure. The reason could also be that there are physisorbed phenoxy mercaptoundecane molecules on the SAM. Hydrophobic interaction between the phenoxy tail groups could make these molecules difficult to remove by ethanol washing and ultrasonication. To improve dissolution of the hydrophobic alkanethiols, it is recommended to evaluate THF as a solvent.



**Scheme 1.** Synthesis of 11-phenoxy-1-mercaptoundecane. 11-phenoxy-1-undecene is formed through the deprotonation of the hydroxyl group, and subsequent nucleophilic attack with Br as leaving group (1). Azobisisobutyronitril is decomposed by the UV-light from the Hg-lamp, generating free radicals that can react with the undecene double bond, creating a free radical that in turn reacts with the thiol group of the thioacetic acid (2). The base-promoted hydrolysis (3) is carried out in the presence of sodium methoxide and neutralized with acetic acid to give the thiol.

**Table 1.** Resulting static contact angles and ESCA data for hydroxyl-presenting SAMs functionalised after formation, and for the SAM formed from the synthesised phenoxy mercaptoundecane (-OPh). Values of the elements are in mol%.

Sample	$\Theta_s$ (°)	C	O	F	S	Au
-OCH <sub>2</sub> C <sub>6</sub> H <sub>5</sub>	55	40.49	9.28			50.24
-OC <sub>3</sub> F <sub>7</sub>	20					
-OC(O)CF <sub>3</sub>	78	43.24	17.77	9.40		29.60
-OC(O)C <sub>3</sub> F <sub>7</sub>	76	34.21	9.84	26.14		29.81
-OPh	50	29.71	10.84		4.03	55.42

The ESCA data in table 1 indicates the expected presence of carbon, oxygen, fluorine and gold on the produced surfaces. All elements with visible peaks in the scanned energy spectrum were included in the reported values. No sulphur was detected on any of the SAMs in this study, except for the OPh surface, even though each alkanethiol is attached to the surface through an S-Au bond. This can be explained by the relatively low atomic sensitivity factor (ASF) of sulphur (0.426), and the fact that the sulphur is located close to the gold layer and hence is partly shielded by the alkyl chain. Gold, with an ASF of 6.805 is easily detected by ESCA in spite of shielding effects.

#### 4.1.2 Synthesis of heptafluorobutoxy mercaptoundecane

In the synthesis of heptafluorobutoxy mercaptoundecane the yield obtained was too low for the product to be analysed with NMR. The separation of the formed substances proved to be difficult. One probable by-product is methoxy-undecene. Heptafluoro butanol is less acidic than phenol, which facilitates the competing deprotonation and nucleophilic reaction with methanol. An optimisation of the reaction conditions is therefore needed. An aprotic solvent such as THF or DMF might be preferable in this case. The use of a more acidic fluorinated alcohol should also be considered as an alternative, e.g. heptafluoro propanol where the electronegative fluoride atoms are situated closer to the hydroxyl group. Due to lack of time, no optimisation of the reaction conditions of the synthesis was performed in the present study.

## 4.2 Introduction of hydrophobic tail groups on hydroxylated SAMs

### 4.2.1 Introduction of aromatic tail groups

As an alternative course of action to the time consuming synthesis of the 11-phenoxy-1-undecane, aromatic groups were introduced on a hydroxyl-presenting SAM through alkylation reaction with benzylbromide (scheme 2). ESCA data for the resulting surface is shown in table 1 (-OCH<sub>2</sub>C<sub>6</sub>H<sub>5</sub>). The alkylation reaction resulted in an increase in the static contact angle from 10° to 55°, indicating that incorporation of aromatic tail groups had occurred. This is comparable to the static contact angle obtained for the SAM of 11-phenoxy-1-undecane (50°). However, advancing contact angles of 85° for surfaces with full coverage of aromatic tail groups (-OPh) have previously been reported by Sigal et al [17].

The somewhat low contact angle obtained in the surface synthesis indicates that the yield of aromatic groups was incomplete. The surface synthesis could probably be further optimised. DMF, which is an aprotic solvent, increases the rate of the  $S_N2$  reaction by raising the energy of the nucleophile. Therefore, the most probable cause of the incomplete conversion of tail groups is the poor accessibility of the nucleophile. This can be improved through changes in reaction conditions such as solvent, temperature, and mixing.

A complication in the on-surface synthesis procedure is that the starting material, i.e. the hydroxylated SAM is quite sensitive and could easily be damaged if a magnetic stirrer was to be used to enhance the mixing. A stronger base should also be considered to enhance the deprotonation of the hydroxyl groups. The alkylation reaction was run with huge excess of NaH and benzylbromide compared to the estimated quantity of hydroxyl groups at the surface ( $\sim 1 \text{ nmol/cm}^2$ ). Even though some of the excess NaH is most likely consumed by water remaining in the previously dried solvent, the amounts of the reactants can be reduced without affecting the yield.

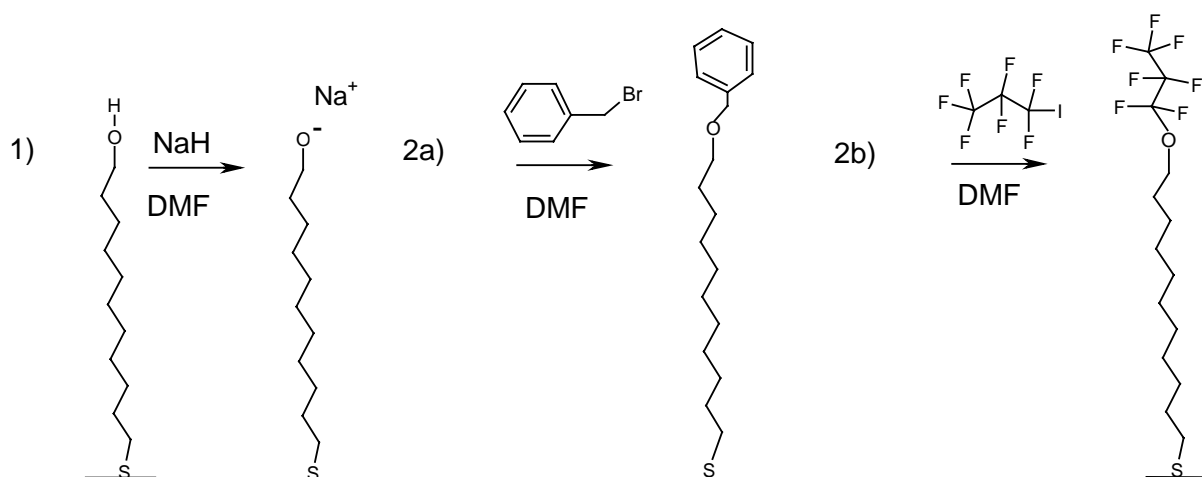
## 4.2.2 Introduction of fluorinated tail groups

### 4.2.2.1 Surface synthesis with heptafluoropropyl iodide

The alkylation reaction with heptafluoropropyl iodide (HFI; scheme 2) was run with an excess of the added reactants similar to the conditions in the reaction with benzylbromide.

Contact angle measurements of the hydroxyl-presenting SAM after reaction with HFI showed an increase from  $10^\circ$  to  $20^\circ$ , implying that no incorporation of fluorinated tail groups had occurred. Due to the low boiling point ( $40^\circ\text{C}$ ) of heptafluoropropyl iodide, the solution could not be heated. THF was tried as an alternative solvent, but it evaporated when the reaction was run at room temperature. To enhance mixing, and avoid problems with evaporation the alkylation reactions should be run under reflux. A stronger base would most likely also increase the yield.

Incorporation of fluorinated groups could also be more successful using a different fluorinated iodide, with at least one methylene unit separating the iodide and the fluorinated chain in the  $S_N2$  reaction. Iodide is normally an excellent leaving group. With HFI, the substrate carbon is situated in an environment that might be too electron rich for an effective nucleophilic substitution to occur. The substitution reaction could also be sterically hindered by the fluorine atoms.

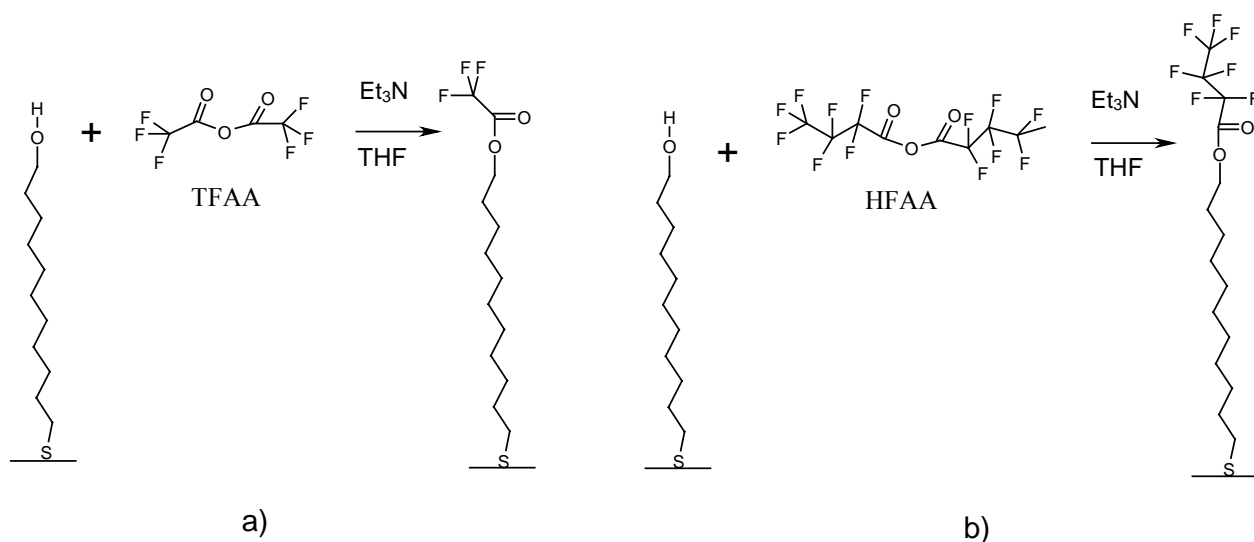


**Scheme 2.** The alkylation reaction. The hydroxylated alkanethiol is first deprotonated (1). It is then allowed to participate in a nucleophilic substitution reaction with either benzyl bromide (2a) with Br as the leaving group, or heptafluoropropyl iodide (2b) with I as the leaving group.

#### 4.2.2.2 Surface synthesis with fluorinated anhydrides

On-surface synthesis with fluorinated anhydrides on SAMs with hydroxyl and carboxyl groups respectively has been proposed as a strategy for the generation of functionalised SAMs [16, 18]. In the present study SAMs formed from 11-mercapto-1-undecanol were reacted with fluorinated anhydrides (TFAA and HFAA respectively) to obtain fluorinated surfaces (scheme 3). Contact angle measurements and ESCA analysis indicated successful introduction of fluorinated tail groups (table 1). As can be expected, the fluorine/carbon ratio on the HFAA surface was significantly higher than on the TFAA surface. Contact angle measurements immediately after the reaction with TFAA showed an increase in contact angle from  $10^\circ$  to  $80^\circ$ . However, the trifluoromethyl ester seemed to be somewhat unstable when stored in ethanol. After 48h in ethanol no fluorine could be detected with ESCA. The ESCA data for TFAA in table 1 was obtained on surfaces that were stored under dry conditions after the reaction. The heptafluoropropyl ester was more stable when stored in ethanol, and significant incorporation of fluorinated groups was detected by ESCA after 48h of ethanol storage. Due to lack of time, comparative dry-storage ESCA measurements could not be performed with the heptafluoropropyl ester surfaces.

The advancing and receding contact angles of the trifluoromethyl ester surface (after dry storage) were measured. The resulting  $\theta_a = 95^\circ$ , and  $\theta_r = 55^\circ$  give a hysteresis of  $40^\circ$ , which is comparable to the hysteresis of  $31^\circ$  ( $\theta_a = 96^\circ$ ,  $\theta_r = 61^\circ$ ) previously reported by Lestelius et al for a similar surface  $(\text{HS}(\text{CH}_2)_{16}\text{OCOCF}_3)$  [16]. The larger hysteresis implies that the reaction yield was lower in the present study, resulting in a less homogenous surface. The quality of the fluorinated monolayer is affected by the quality of the starting material, i.e. the hydroxylated SAM, and by the accessibility of the hydroxyl groups at the surface.



**Scheme 3.** Introduction of fluorinated tail groups on a hydroxyl-presenting SAM. The exposed hydroxyl groups readily reacts with the anhydride, with triethyl amine as a catalyst, to form trifluoromethyl ester (a) and heptafluoropropyl ester (b) respectively.

### 4.3 Mixed monolayers of hydrophilic and hydrophobic alkanethiols

In the monolayers previously discussed in this report, the chemistry, structure and properties of the surfaces were controlled by varying the tail group, either before or after the SAM formation. However, the range of properties that can be obtained in homogenous monolayers of a single thiol is limited. Greater variation of the SAM structure is afforded by coadsorption of two or more thiols that differ in the nature of the tail group. Figure 5 shows the resulting static contact angles of SAMs formed from two-component ethanol solutions of 1-undecanethiol and 11-mercapto-1-undecanol, with the molar fraction in solution of the polar component ( $X_{\text{sol}}^{\text{OH}}$ ) varying from 0 to 1. The relationship between the composition of the solution and the composition of the resulting monolayer for the hydroxyl/methyl system has previously been investigated by Bain et al [19]. They found that adsorption of the component with the polar tail group was disfavoured at low concentrations in solution. The results in figure 5 are in accordance with these findings. ESCA data for some of the mixed SAMs show that the fraction of oxygen on the surface compared to carbon (O/C) increases with the fraction in solution of the polar component (table 2; figure 6).

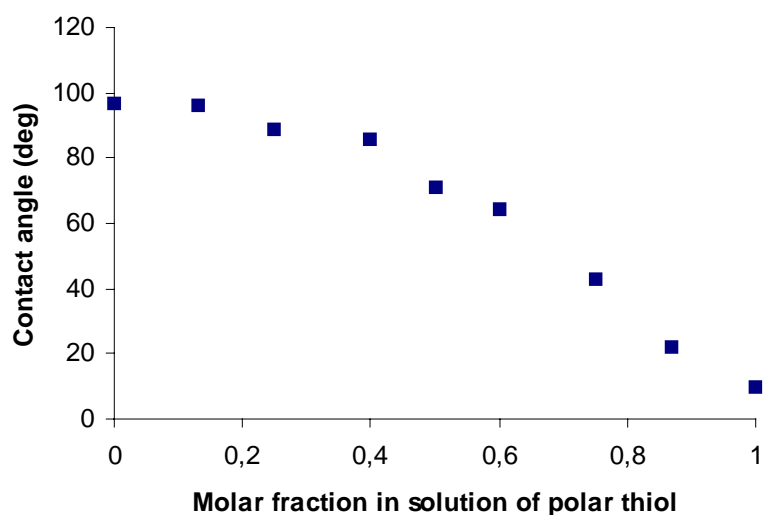


**Figure 5.** Resulting contact angles of water on mixed monolayers (OH/CH<sub>3</sub>) formed from ethanol solutions with varying molar fraction in solution of the polar component.

**Table 2.** ESCA data for mixed monolayers. -OH and -CH<sub>3</sub> denote single-component SAMs of 11-mercapto-1-undecanol and 1-undecanethiol respectively. Numbers 0.25-0.75 denote molar fraction in solution of -OH. Values of the elements are in mol%.

Sample	C	O	Au
-CH <sub>3</sub>	56.75		43.25
0.25	51.72	2.46	45.82
0.5	54.61	3.17	42.21
0.75	43.49	6.19	42.43
-OH	53.37	7.41	39.21

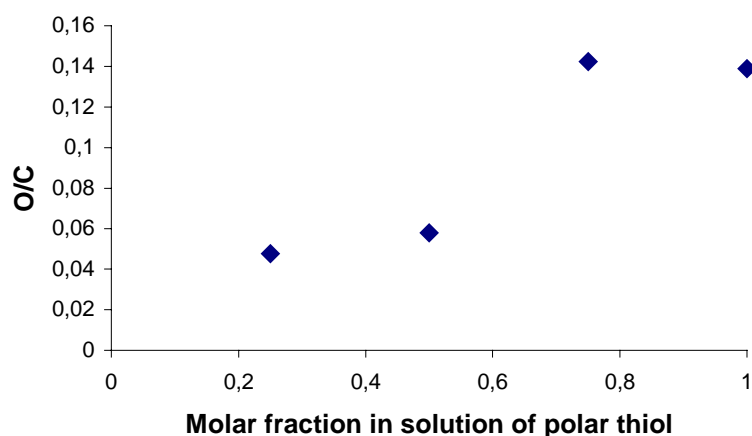


**Figure 6.** Resulting oxygen/carbon ratios (*O/C*) as measured by ESCA on mixed monolayers (*OH/CH<sub>3</sub>*) formed from ethanol solutions with varying molar fraction in solution of the polar component.

Thiols are readily oxidised to disulphides, and the adsorption kinetics of disulphides is slower than for the corresponding thiols. This proved to be an important factor when studying mixed monolayers. After three months of usage of the polar component 11-mercapto-1-undecanol, the contact angles of the produced mixed monolayers ( $>70^\circ$  for all  $X_{sol}^{OH}$ ) indicated that there had been significant oxidation of the polar thiol, in spite of storage under N<sub>2</sub>. At this stage, the mixed monolayers appeared to be totally dominated by the non-polar component, most likely due to the even more kinetically disfavoured adsorption of disulphides compared to thiols. The solubility in ethanol of the polar component had also decreased dramatically.

#### 4.4 Characterisation of produced SAMs

Table 3 summarises the methods used in the characterisation of the SAMs in this study. Contact angle measurements were performed on all surfaces. A selection of surfaces were analysed with the other methods.

**Table 3.** Static contact angles ( $\theta_s$ ), and extent of further characterisation of SAMs formed from the various alkanethiols, (+ indicates that analysis was performed).

<i>Sample</i>	<i>Tail group</i>	$\theta_s$ (deg)	<i>ESCA</i>	<i>SPR</i>	<i>MALDI-MS</i>
Perfluorodecanethiol	-C <sub>8</sub> F <sub>17</sub>	110			+
Octadecylmercaptan	-CH <sub>3</sub>	104			
1-Hexadecanethiol	-CH <sub>3</sub>	100		+	+
1-Undecanethiol	-CH <sub>3</sub>	97	+		
11-Phenoxy-1-mercaptoundecane	-OPh	50	+	+	+
11-Mercaptoundecanoic acid	-COOH	15			
11-Mercapto-1-undecanol	-OH	10	+	+	+
Trifluoromethyl ester	-OC(O)CF <sub>3</sub>	78	+		
Heptafluoropropyl ester	-OC(O)C <sub>3</sub> F <sub>7</sub>	76	+		
Benzyl on OH	-OCH <sub>2</sub> C <sub>6</sub> H <sub>5</sub>	55	+		
Mixed OH/CH <sub>3</sub>	OH/CH <sub>3</sub>	figure 5	+		

SAMs formed from thiol solution were produced with static contact angles ranging from 10° to 110° (table 3). Advancing ( $\theta_a$ ) and receding ( $\theta_r$ ) contact angles for some of the surfaces are presented in table 4, together with the calculated hysteresis ( $\theta_a - \theta_r$ ) of the surfaces. For the hydrophobic surfaces, the advancing contact angles reported here are somewhat ( $\leq 5^\circ$ ) lower than values commonly found in literature. One explanation for this could be that the gold substrate surfaces used in the present study exhibit a higher roughness. The best SAMs produced in the present study exhibit hysteresis of 17°.

**Table 4.** Advancing ( $\theta_a$ ) and receding ( $\theta_r$ ) contact angles of SAMs formed from the various alkanethiols.

<i>Sample</i>	$\theta_a$	$\theta_r$	$\theta_a - \theta_r$
Perfluorodecanethiol	115	95	20
1-Hexadecanethiol	107	90	17
1-Undecanethiol	104	86	18
11-Phenoxy-1-mercaptoundecane	68	35	33

## 4.5 Adsorption of proteins and peptides

SPR and MALDI-MS have previously been shown to be convenient methods for the detection of protein and peptide adsorption respectively [6, 17, 20]. To characterise the monolayers produced in the present study with respect to their affinity for proteins and peptides both methods were used. With SPR, the unspecific adsorption of a selection of small, large, and intermediate size proteins, and a three-component peptide sample was monitored. Peptide adsorption to the SAMs was detected using MALDI-MS.

### 4.5.1 Protein adsorption studied with SPR

Adsorption of proteins and peptides was studied through SPR measurements on SAMs of 1-hexadecanethiol (CH<sub>3</sub>), 11-phenoxy-1-mercapto undecane (OPh), and 11-mercapto-1-undecanol (OH) respectively. As model proteins for the adsorption studies BSA, lysozyme and fibrinogen, three well-characterized proteins of different sizes were chosen (table 5). Each protein was passed separately over the studied surface. The resulting adsorption behaviour and surface concentrations for the proteins are shown in figures 7-9. Due to lack of time, each surface/protein combination was only tested once. The injection series of lysozyme on the OH SAM (figure 8) was prematurely interrupted due to an air bubble in the sample disrupting the measurement after the third injection.

Consistently with earlier studies of these and similar systems [16, 17, 20], lysozyme adsorbed better to OPh surfaces than to OH surfaces. BSA adsorbed better than lysozyme to all surfaces. Fibrinogen exhibited a higher surface density than BSA on the hydrophobic surface. An unexpected result was that BSA exhibited equally strong adsorption to the hydrophilic OH surface as it did to the OPh surface. A possible explanation of this result is that the high-energy OH surface had been damaged or contaminated prior to the measurements.

These protein and surface combinations have previously been investigated by Sigal et al [17]. It was then found that small proteins (e.g. lysozyme) are extremely sensitive to the wettability of the surface. They adsorb well to the surfaces presenting CH<sub>3</sub> and OPh groups, and very little to hydroxyl presenting surfaces. Lysozyme has a strong structural stability, and electrostatic repulsion is generally more important for the weak adsorption on hydrophilic surfaces than are structural rearrangements [21]. In the study by Sigal et al, BSA, which is of intermediate size, proved to be less sensitive to wettability, but exhibit limited adsorption to OH-presenting surfaces. On the phenoxy-presenting surface,  $\pi$ - $\pi$  interactions between the  $\pi$  electrons in the protein and the  $\pi$  electrons of the phenol ring contribute to the extensive adsorption. Large proteins, such as fibrinogen are less sensitive to surface wettability than smaller proteins. The high molecular weight proteins interact strongly with the surface due to increased multipoint attachments and, as a consequence have higher binding energies to the surface. Fibrinogen adsorbs well even to the most hydrophilic surfaces. The stronger adhesion forces of fibrinogen to both CH<sub>3</sub> and OH presenting SAMs compared to those exhibited by albumine to the same surfaces have also been observed by Kidoaki et al [22].

**Table 5.** Molecular weights, isoelectric points and theoretical monolayer densities of proteins studied with SPR.  $\Gamma_{side}$  and  $\Gamma_{end}$  denote that the long axis of the protein is oriented parallel and perpendicular to the surface respectively [17].

<i>Protein</i>	<i>MW (kD)</i>	<i>pI</i>	<i><math>\Gamma_{side}</math> (ng/cm<sup>2</sup>)</i>	<i><math>\Gamma_{end}</math> (ng/cm<sup>2</sup>)</i>
Fibrinogen	340	5.5	240	2400
Bovine serum albumin (BSA)	69	4.8	250	600
Lysozyme	14	11.1	170	260

The observed adsorption kinetics for the protein measurements in this study were much slower than expected, especially the kinetics for the adsorption of BSA to CH<sub>3</sub> (figure 9-10). An explanation of this is the suspected presence of a surfactant (P20), which is commonly used in the BIAcore instrument, and that might have prevailed in the system in spite of the performed desorption procedure with SDS prior to the measurement. Additionally, the process of protein adsorption is very complex and involves many sub-processes such as protein-interface interactions, protein reorientation, conformational changes accompanied by protein unfolding, lateral protein-protein interactions and desorption, resulting in multiple states of adsorbed proteins on the surface. Passing PBS over the surface in-between the relatively short sample injections most likely affects the rate of protein adsorption, as well as the characteristics of the resulting protein layer. The proteins that have reached the surface and adsorbed during a sample injection have time to relax at the interface before the next protein sample is injected. The initial protein footprints of albumine and fibrinogen have been shown to grow with up to a factor of 5 as the protein relaxes [23]. The interfacial relaxation thus determines the ultimate coverage of the surface. This would also explain the relatively low adsorption of BSA to the hydrophobic CH<sub>3</sub> surface. For comparison, the theoretical surface densities of a complete monolayer of the studied proteins are listed in table 5. To obtain quantitative data describing the protein adsorption, continuous sample injection would be preferable.

The SPR response ( $\Delta\theta_m$ ) due to the adsorption of proteins or peptides is given by the BIAcore instrument software expressed in resonance units (RU), where 1RU corresponds to a change in  $\theta_m$  of  $10^{-4}^\circ$ . An example of the sensorgrams obtained with BIAcore is shown in figure 10. It corresponds to the adsorption values plotted in figure 9 (truncated after eight injections). To compensate for baseline drift, 1RU/100s was subtracted from the obtained values. The reported quantity of adsorbed protein molecules per unit of surface area ( $\Gamma$ , in units of ng/cm<sup>2</sup>) was calculated according to equation 3 [17].

$$\Gamma \text{ (ng/cm}^2\text{)} = 900\text{(ng/(deg cm}^2\text{))} \times \Delta\theta_m \quad (3)$$

#### 4.5.2 Peptide adsorption studied with SPR

The injected peptide solution contained all three peptides (table 6). No adsorption could be detected when peptide solution was injected over the OPh and CH<sub>3</sub> SAM respectively. According to the manufacturer, the BIAcore system allows detection of direct adsorption of molecules down to a molecular weight of around 2000D. The peptides studied in the present report are most likely too small even for measurements of unspecific adsorption, especially when studying a two-dimensional surface. Additionally, the adsorption time used in the measurements was probably too short for sufficient adsorption to occur. Due to the limited available quantities of peptides the injected peptide solution was more dilute than the protein solutions, and the adsorption time was shortened to 12 minutes (2x30 $\mu$ l injections separated by 1 minute of PBS). The detection limit of the BIAcore system is 1ng/cm<sup>2</sup> according to the manufacturer, but factors such as background noise and baseline stability affect the sensitivity.

**Table 6.** Molecular weights and isoelectric points of peptides studied with SPR.

Peptide	MW (D)	pI
Angiotensin I	1296.4	6.92
Neuropeptide Y	2657.8	4.11
Ile-Ser-bradykinin	1260.4	12.0

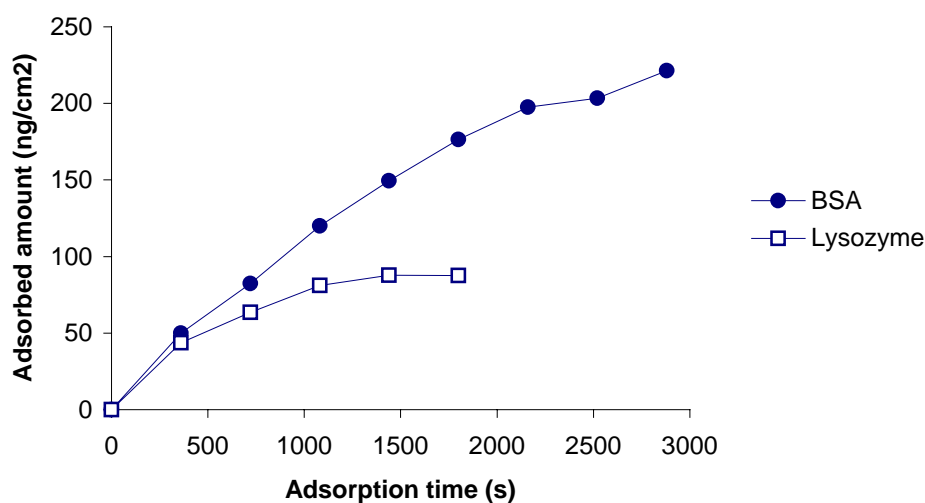


**Figure 7.** Adsorption of BSA and lysozyme on a SAM of 11-phenoxy-1-undecane. Each data point represents the adsorbed amount after a 6 min sample injection, followed by 1 min of passing PBS over the surface.

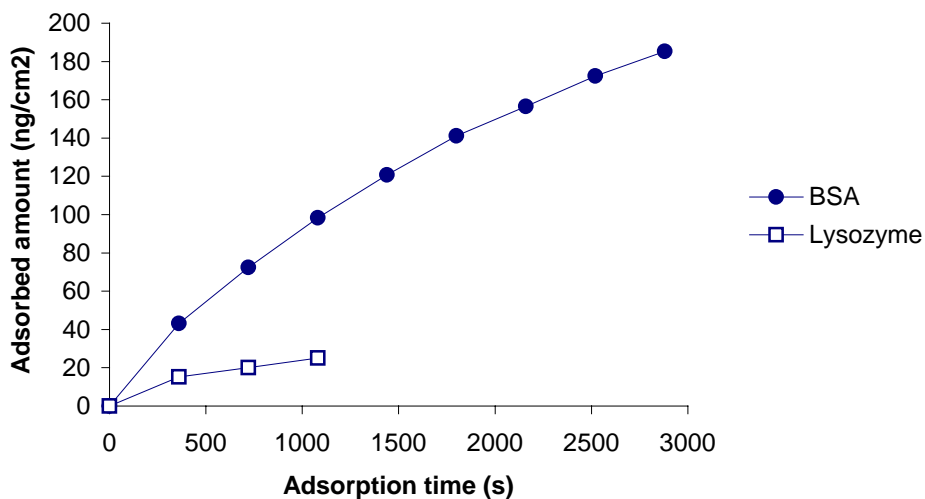


**Figure 8.** Adsorption of BSA and lysozyme on a SAM of 11-mercapto-1-undecanol. Each data point represents the adsorbed amount after a 6 min sample injection, followed by 1 min of passing PBS over the surface.

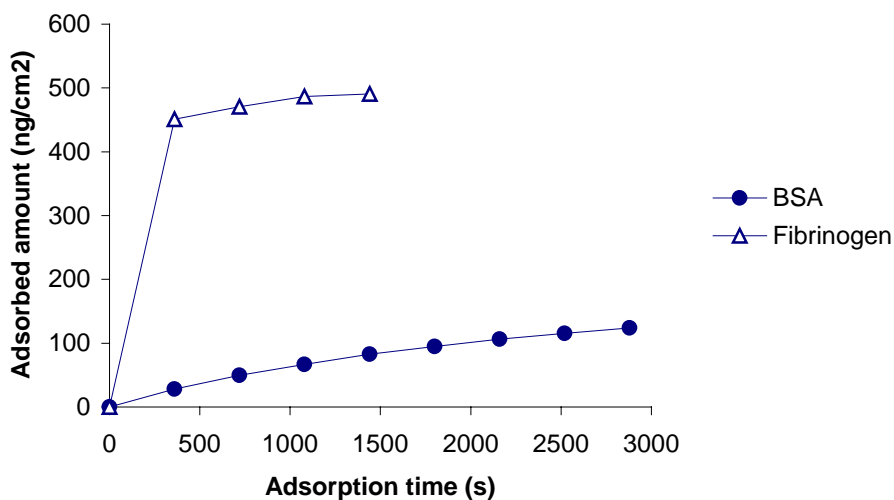


**Figure 9.** Adsorption of BSA and fibrinogen on a SAM of 1-hexadecanethiol. Each data point represents the adsorbed amount after a 6 min sample injection, followed by 1 min of passing PBS over the surface.

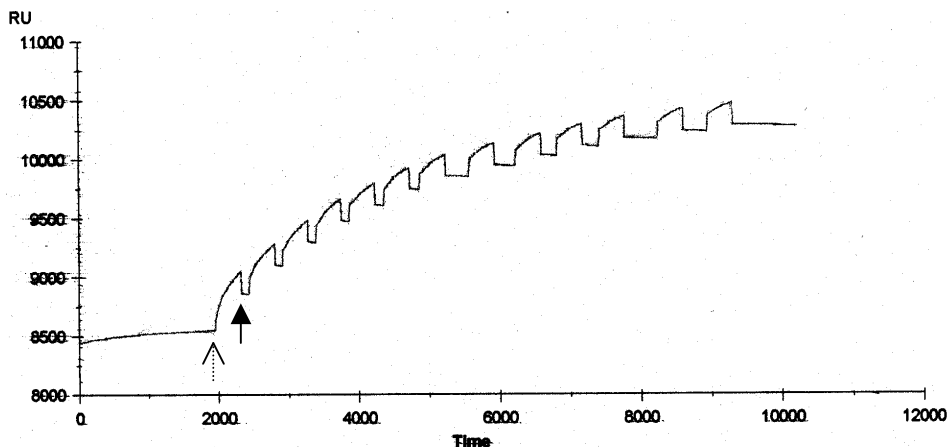


**Figure 10.** Sensorgram obtained for the adsorption of BSA to a SAM of 1-hexadecanethiol. The dotted arrow marks the first of 13 BSA injections, and the bold arrow marks the start of the first PBS rinse. The difference in RU between the baseline at the first injection, and the response after the PBS rinse represents the protein adsorption at that time. The increase in RU before the PBS rinse is partly due to the difference in refractive index between the sample and the PBS buffer.

#### 4.5.3 Peptide adsorption studied with MALDI-MS

MALDI-MS is a much more sensitive method than SPR, and was used for the detection of adsorbed peptides. The detection limit with MALDI-MS lies in the attomole to nanomole range. Surfaces included in the MALDI-MS peptide adsorption study are listed in table 7.

The MALDI-MS measurements indicated various degrees of peptide adsorption to all surfaces. The strongest signals were obtained from the 11-phenoxy-1-mercaptoundecane SAM (OPh), and from the bare gold surface. On the bare gold surface there was a strong peptide signal already after 1 minute of adsorption with subsequent washing. No peptides were detected on the SAM-covered surfaces after 1 minute of adsorption.

The SAMs of hexadecanethiol ( $\text{CH}_3$ ) and perfluorodecane ( $\text{F}_{17}$ ) exhibited somewhat lower degrees of peptide adsorption than the OPh SAM after 10 minutes (figures 11-13). On the most hydrophilic surface (11-mercapto-1-undecanol) spectroscopic measurements proved to be very difficult due to extensive spreading of the matrix over the surface. Four peptides that were detected on two or more of the SAM-covered surfaces are listed in table 8. The peptides are rich in aromatic (F, Y) or neutral hydrophobic amino acids (L, P, V), that could be expected to engage in hydrophobic interactions with e.g. the phenoxy tail groups.

The strong peptide signal on the bare gold surface can partly be explained by the fact that the applied peptide droplet evaporated quickly (in <3 minutes), resulting in the deposition of peptides on the surface. Additionally, the gold surface is most likely highly adsorbing after the plasma cleaning, which would explain that peptides were detected as early as after 1 minute, with no visible evaporation of the droplet. A similar peptide adsorption method was previously tested by Brockman et al [6]. They found that peptides could be detected on the analysed SAM, but that the method has its limitations.

To overcome problems with evaporation, and the limited droplet surface area in contact with the SAM, the optimal method would be to immerse the sample surface in peptide solution for an extended time period (>8h). However, immersion of the sample surface demands large quantities of the studied peptide.

**Table 7.** Static contact angles ( $\Theta_s$ ) of surfaces included in the MALDI-MS peptide adsorption study

Surface	$\Theta_s$ ( $^\circ$ )
Perfluorodecanethiol	110
1-Hexadecanethiol	100
11-Phenoxy-1-mercaptoundecane	50
11-Mercapto-1-undecanol	10
Plasma treated gold	65

**Table 8.** Molecular weight, position, and peptide sequence of peptides adsorbed on the F<sub>17</sub>, OPh and CH<sub>3</sub> SAMs.

MW	Position	Peptide sequence
1567.743	347-359	DAFLGSFLYEYSR
1482.798	483-495	LCVLHEKTPVSEK
1439.812	360-371	RHPEYAVSVLLR
2045.028	168-183	RHPYFYAPELLYYANK

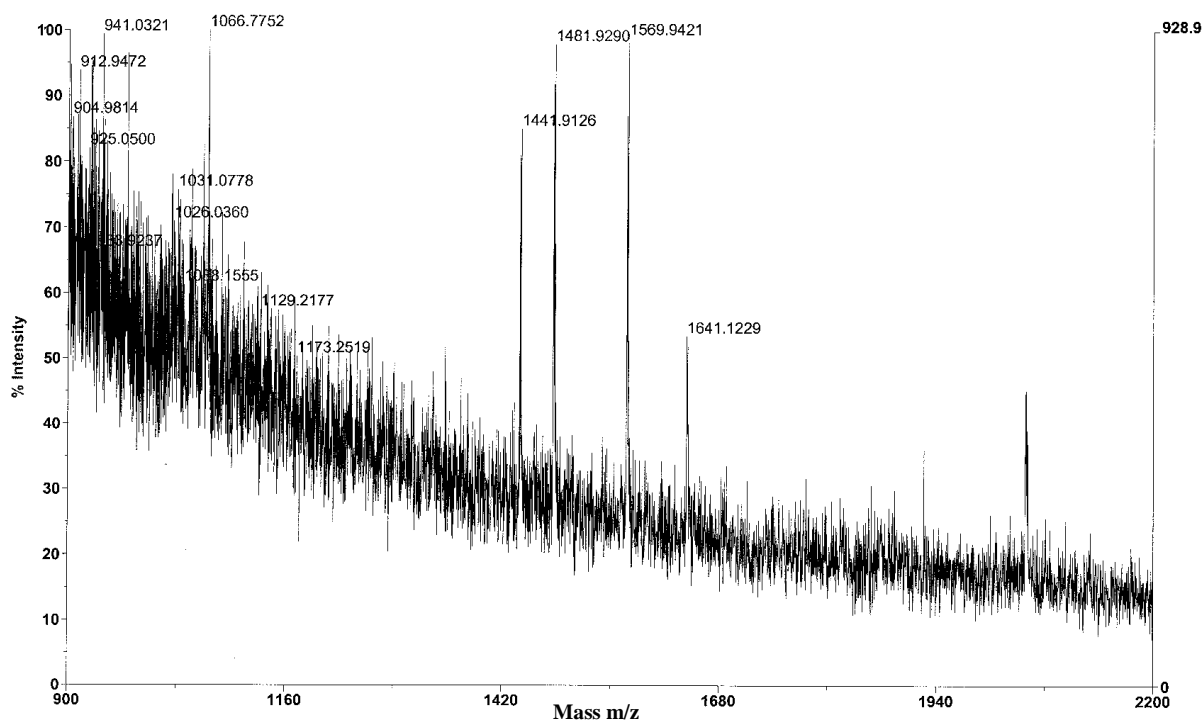


**Figure 11.** MALDI Mass spectrum of BSA Trp-digest on a SAM of perfluorodecane.

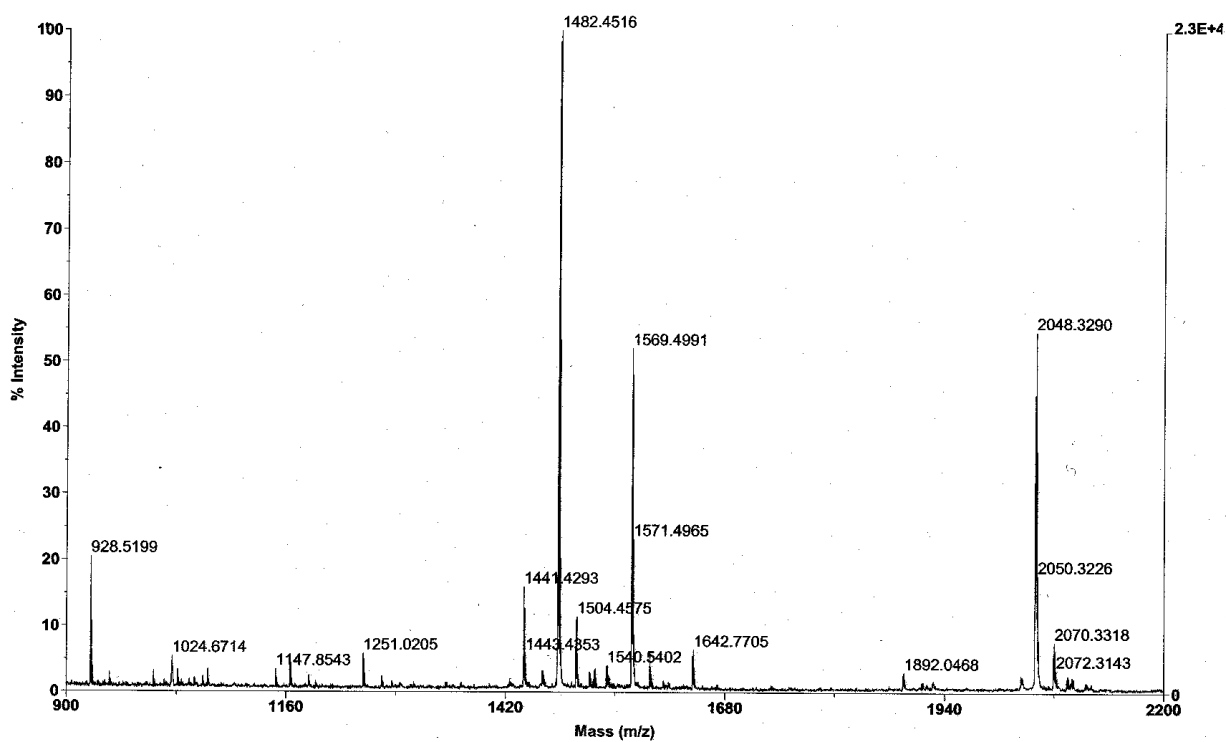


**Figure 12.** MALDI Mass spectrum of BSA Trp-digest on a SAM of 11-phenoxy-1-mercapto undecane.

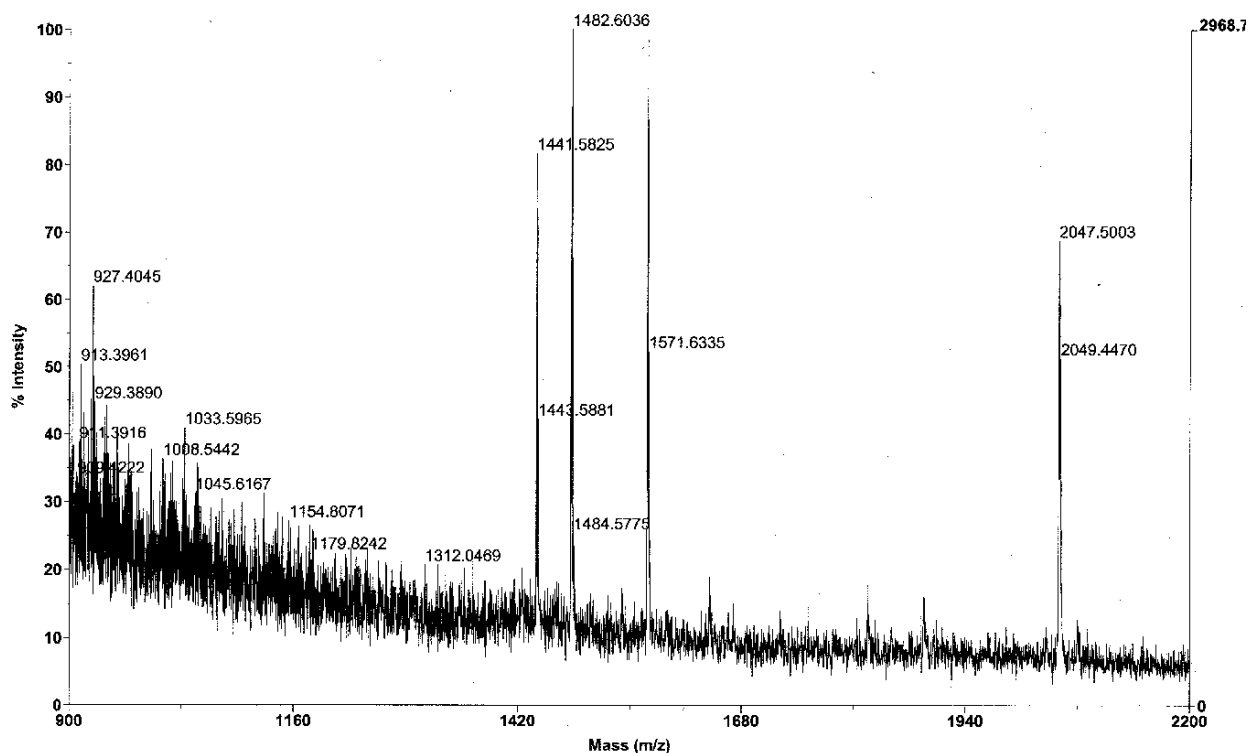


**Figure 13.** MALDI Mass spectrum of BSA Trp-digest on a SAM of hexadecanethiol.

## 5 Conclusions

- The self-assembly of alkanethiols on gold substrate proved to be a convenient method for the production of surfaces exhibiting air-water contact angles ranging from hydrophilic ( $\theta_s \leq 10^\circ$ ) to hydrophobic ( $\theta_s > 90^\circ$ ).
- To increase the variety of surface wettabilities, mixed monolayers of polar and non-polar thiols can readily be produced. Oxidation of the polar thiols proved to be of great importance for the resulting fraction of polar components on the surface.
- The synthesis of an alkanethiol with a phenoxy tail group was performed with a yield of 60% and high purity. A high degree of oxidation of the thiol to the disulphide was observed, but did not impair the formation of the SAM.
- As an alternative to the complete synthesis of substituted alkanethiols, hydrophobic phenoxy or fluorinated tail groups were successfully introduced on the surface of hydroxylated SAMs.
- The protein adsorption studies gave some indications of small proteins being more sensitive than large proteins to surface wettability. The sensitivity of SPR proved to be too low to allow detection of adsorbed peptides under the conditions studied.
- It was found that MALDI-MS could be used to identify peptides deposited on a SAM. Various degrees of peptide adsorption were detected on all investigated surfaces. Among the SAM-covered surfaces the highest peptide signal was obtained from the 11-phenoxy-1-undecane SAM. For more controlled adsorption conditions, sample surfaces should be immersed in peptide solution for an extended time period.

## 6 Proposed future actions

- Optimise the synthesis of heptafluorobutoxy mercaptoundecane, and the surface synthesis with heptafluoropropyl iodide and benzylbromide.
- Investigate the adsorption behaviour of additional combinations of biomolecules and SAMs. Produce SAMs presenting charged tail groups (e.g.  $\text{CO}_2^-$  and  $\text{NH}_3^+$ ) and include them in a peptide/protein affinity study. Perform additional protein/peptide adsorption studies with SPR and MALDI-MS to confirm the results obtained in the present report.
- Investigate the formation of SAMs on other metal surfaces than gold, e.g. Cu or Ag, to decrease production costs for future applications.

## 7 Acknowledgements

First of all, I would like to extend my warmest thanks to everybody at Gyros for making my final project such a fun experience. In particular, I would like to thank Ann-Kristin Honerud, who made me see the beauty of organic chemistry, for her invaluable help, advice, and support throughout the project, and my supervisor Helene Dérand for always being supportive and open-minded. Thanks also to Kurt Nordström and Åsa Rosengren for helping out with the Biacore instrument, Magnus Gustafsson for the MALDI-MS analysis, and Jim Van Alstine for being my examiner.

## References

- 1 Liedberg, B & J.M. Cooper, J.M., *Bioanalytical applications of self-assembled monolayers*. Immobilized biomolecules in analysis: A practical approach. (Ed's: Cass, T. & Lieger, F.S.). Oxford University Press, 1998: 55-78.
- 2 Chapman, R.G., Ostuni, E. & Whitesides, G.M., *Preparation of mixed self-assembled monolayers (SAMs) that resist adsorption of proteins using the reaction of amines with a SAM that presents interchain carboxylic anhydride groups*. Langmuir, 2000. 16: 6927-36.
- 3 Ostuni, E., Yan, L. & Whitesides, G.M., *The interaction of proteins and cells with self-assembled monolayers of alkanethiolates on gold and silver*. Coll. Surf. B: Biointerf., 1999. 15 (1): 3-30.
- 4 Laibinis, P.E., Palmer, B.J., Lee, S-W. & Jennings, G.K., *The synthesis of organothiols and their assembly into monolayers on gold*. Thin films, 1998. 24: 1-41.
- 5 Löfås, S., *Dextran modified self-assembled monolayer surfaces for use in bio interaction analysis with surface plasmon resonance*. Pure & Appl. Chem., 1995. 67 (5): 829-34.
- 6 Brockman, A.H., Dodd, B.S. & Orlando, R., *A desalting approach for MALDI-MS using on-probe hydrophobic self-assembled monolayers*. Anal. Chem., 1997. 69: 4716-20.
- 7 Bain, C.D., Troughton, E.B., Tao, Y-T., Evall, J., Whitesides, G.M. & Nuzzo, R.G., *Formation of monolayer films by the spontaneous assembly of organic thiols from solution onto gold*. J. Am. Chem. Soc., 1989. 111: 321-35.
- 8 Dubois, L.H. & Nuzzo, R.G., *Synthesis, structure, and properties of model organic surfaces*. Annu. Rev. Phys. Chem., 1992. 43: 437-63.
- 9 Laibinis, P.E., Whitesides, G.M., Allare, D.L., Tao, Y-T., Parikh, A.N. & Nuzzo, R.G., *Comparison of the structures and wetting properties of self-assembled monolayers of n-alkanethiols on the coinage metal surfaces, Cu, Ag, Au*. J. Am. Chem. Soc., 1991. 113: 7152-67.
- 10 Laibinis, P.E. & Whitesides, G.M.,  *$\omega$ -terminated alkanethiolate monolayers on surfaces of copper, silver, and gold have similar wettabilities*. J. Am. Chem. Soc., 1992. 114 (6): 1990-95.
- 11 Bain, C.D., Biebuyck, H.A. & Whitesides, G.M., *Comparison of self-assembled monolayers on gold: Coadsorption of thiols and disulfides*. Langmuir, 1989. 5: 723-27.
- 12 Bertilsson, L. & Liedberg, B., *Infrared study of thiol monolayer assemblies on gold: preparation, characterization, functionalisation of mixed monolayers*. Langmuir, 1993. 9: 141-49.

- 13 Ron, H. & Rubinstein, I., *Alkanethiol monolayers on preoxidized gold. Encapsulation of gold oxide under an organic monolayer*. Langmuir, 1994. 10: 4566-73.
- 14 Ron, H., Matlis, S. & Rubinstein, I., *Self-assembled monolayers on oxidized metals. 2. Gold surface oxidative pre-treatment, monolayer properties, and depression formation*. Langmuir, 14 (5): 116-21.
- 15 Liedberg, B. & Johansen, K., *Affinity bio sensing based on surface plasmon resonance detection. From: Methods in biotechnology*. Affinity biosensors: Techniques and protocols. (Ed's: Rogers, K.R. & Mulchandani, A.). Humana Press Inc., Totowa, NJ. Vol. 7: 31-35.
- 16 Lestelius, M., Liedberg, B. & Tengvall, P., *In vitro plasma protein adsorption on  $\omega$ -functionalized alkanethiolate self-assembled monolayers*. Langmuir, 1997. 13: 5900-08.
- 17 Sigal, G.B., Mrksich, M. & Whitesides, G.M., *Effect of surface wettability on the adsorption of proteins and detergents*. J. Am. Chem. Soc., 1998. 120: 3464-73.
- 18 Yan, L., Marzolin, C., Terfort, A. & Whitesides, G.M., *Formation and reaction of interchain carboxylic anhydride groups on self-assembled monolayers on gold*. Langmuir, 1997. 13, 6704-12.
- 19 Bain, C.D., Evall, J. & Whitesides, G.M., *Formation of monolayers by the coadsorption of thiols on gold: Variation in the head group, tail group, and solvent*. J. Am. Chem. Soc., 1989. 111: 7155-64.
- 20 Silin, V., Weetall, H. & Vanderah, D.J., *SPR studies of the nonspecific adsorption kinetics of human IgG and BSA on gold surfaces modified by self-assembled monolayers (SAMs)*. J. of colloid and interface science, 1997. 185: 95-103.
- 21 Ball, V. & Ramsden, J.J., *Absence of surface exclusion in the first stage of lysozyme adsorption is driven through electrostatic self-assembly*. J. Phys. Chem. B., 1997. 101 (28): 5465-69.
- 22 Kidoaki, S. & Matsuda, T., *Adhesion forces of the blood plasma proteins on self-assembled monolayer surfaces of alkanethiolates with different functional groups measured by an atomic force microscope*. Langmuir, 1999. 15: 7639-46.
- 23 Wertz, C.F. & Santore, M.M., *Adsorption and relaxation kinetics of albumin and fibrinogen on hydrophobic surfaces: Single-species and competitive behavior*. Langmuir, 1999. 15: 8884-94.

Appendix 1. <sup>1</sup>H-NMR of the synthesised 11-phenoxy-1-mercaptoundecane

